

# A Hybrid Evolutionary Algorithm, Utilizing Novelty Search and Local Optimization, Used to Design Convolutional Neural Networks for Handwritten Digit Recognition

Tabish Ashfaq, Nivedha Ramesh and Nawwaf Kharm

*Department of Electrical and Computer Engineering, Concordia University, Montreal, Quebec, Canada*

**Keywords:** Neuroevolution, Evolutionary Algorithms, Convolutional Neural Networks, Deep Learning, Cartesian Genetic Programming, Genetic Algorithms, Stochastic Local Search, Novelty Search, Simulated Annealing.

**Abstract:** Convolutional neural networks (CNNs) are deep learning models that have been successfully applied to various computer vision tasks. The design of CNN topologies often requires extensive domain knowledge and a high degree of trial and error. In recent years, numerous Evolutionary Algorithms (EAs) have been proposed to automate the design of CNNs. The search space of these EAs is very large and often deceptive, which entails great computational cost. In this work, we investigate the design of CNNs using Cartesian Genetic Programming (CGP), an EA variant. We then augment the basic CGP with methods for identifying potential/actual local optima within the solution space (via Novelty Search), followed by further local optimization of each of the optima (via Simulated Annealing). This hybrid EA methodology is evaluated using the MNIST data-set for handwritten digit recognition. We demonstrate that the use of the proposed method results in considerable reduction of computational effort, when compared to the basic CGP approach, while still returning competitive results. Also, the CNNs designed by our method achieve competitive recognition results compared to other neuroevolutionary methods.

## 1 INTRODUCTION

Image recognition is a widely studied application of computer vision. In recent years Convolutional Neural Networks (CNNs) have proven to be especially effective at this task in a supervised learning context. This has motivated the development of numerous evolutionary algorithms (EAs) for the design of CNN architectures and for the optimization of their hyperparameters (Baldominos et al., 2018; Xie and Yuille, 2017; McGhie et al., 2020).

The computational effort expended by such algorithms in obtaining optimal solutions is considerable, and thus, such an approach may not be a viable option when computational resources are constrained. As with many applications of evolutionary computing, a large proportion of the computational effort is expended in evaluating a population of individual solutions, many of which may be highly unfit or simply redundant. As such, if a candidate solution is determined (by some criteria) to be useless, it may be removed from the population, which saves on computational time without degrading the effectiveness of evolutionary search and optimization.

Therefore, we are motivated to investigate modifications to the standard evolutionary approach which may lead to a more efficient neural architecture search procedure. This implies that potential solutions to the problem should aim to reduce the number of wasted cycles in the evolution process. This may be done by identifying local optima within the solution space and restricting the search to the neighbourhoods of these local optima. For this purpose, we present a method for approximate quantification of structural diversity and for characterization of local neighbourhoods within a population of CNNs.

In this work, we investigate the use of a three-stage evolutionary optimization approach. The first stage in this approach aims to generate a diverse initial generation of CNNs using the Novelty Search algorithm (Lehman and Stanley, 2011). The second stage involves the evolution of CNN architectures using Cartesian Genetic Programming (CGP) (Miller and Thomson, 2000). In the third stage, we select the most diverse generation from the previous stage. From this population, we sample the most optimal individuals in terms of both fitness and novelty, using a multi-objective optimization algorithm. We attempt

to exploit the local neighbourhoods of these individuals using a stochastic local search (SLS) algorithm. The SLS algorithm implemented for this paper is the Simulated Annealing (SA) (Kirkpatrick et al., 1983) algorithm.

The rest of this paper is organised as follows. Section 2 provides a review of related work in neuroevolution. Section 3 describes the genetic encoding, and our optimized evolutionary approach to designing CNN architectures. We present the results of our proposed methodology in Section 4. Finally, we end with some concluding remarks and recommendations for future work in Section 5.

## 2 RELATED WORK

Neuroevolution has been used to design various types of neural network weights and topologies to address a wide range of problems. In 2002, the highly influential technique, Neuroevolution of Augmenting Topologies (NEAT) (Stanley and Miikkulainen, 2002), was developed and proved effective in evolving the architecture and weights of small neural networks. In 2009, this method was extended with the introduction of the HyperNEAT algorithm (Stanley et al., 2009), which allowed for the evolution of larger scale neural networks through indirect encoding using a Compositional Pattern Producing Network (CPNN). However, this technique has been shown to be ineffective in performing image classification, and has resulted in an error rate of 7.9% on the MNIST dataset when used for feature learning with a CNN (Verbancsics and Harguess, 2015).

In recent years, several works have been published which attempt to automate the design of CNNs through neuroevolution. Genetic CNN (Xie and Yuille, 2017) is a Genetic Algorithm which uses a fixed-length binary string representation. The authors obtained competitive recognition results on the MNIST dataset. However, they do not encode the fully-connected part of the network, choosing to adapt the fully-connected part of the basic LeNet architecture (Lecun et al., 1998).

Baldominos et al. (Baldominos et al., 2018) studied the evolution of CNNs using both a GA with binary Gray encoding representation, as well as Grammatical Evolution which uses an integer-based encoding. They include both convolutional and fully-connected components in their frameworks, in addition to parameterizing the connectivity pattern within the networks, thereby allowing for the evolution of recurrent structures. The authors also present a similarity metric which they use to implement a niching

strategy. However, the metric presented in this paper evaluates to zero for individuals with unequal numbers of convolutional and dense layers, and hence, it does not provide a measure of similarity in many cases.

Sun et al. (Sun et al., 2020) propose a GA which encodes highly functional blocks in variable-length chromosomes, and incorporates skip connections. Similarly, a CGP-based approach (Suganuma et al., 2017) was published in 2017 which uses a function set of convolutional and residual units to reduce the search space. In both of these cases, only the convolutional part of the network is encoded. In addition, these works do not attempt to measure structural similarity between different neural networks. In this work, we augment the CGP approach introduced by Suganuma et al. by extending the function set and incorporating transpose convolutions and fully connected layers.

## 3 METHODS

We evolve two separate populations of CNNs. The first of these populations, is optimized according to the fitness criteria described in Section 3.2.2, beginning with a randomly generated initial generation. This population is henceforth referred to as Population 1. In the second population, Population 2, as an alternative to random initialization, we include a distinct initialization stage. In this stage, we begin with a randomly generated population and optimize it for novelty, using the Novelty Search algorithm (Lehman and Stanley, 2011) along with the metric developed in Section 3.3. This process yields the initial generation for the evolutionary algorithm. Lastly, we apply a different survivor selection scheme during evolution of each of the two populations, as described in Section 3.2.3.

The individual networks evolved in our algorithms are each designed as a combination of two sub-networks: a fully convolutional network followed by a fully connected (dense) network.

### 3.1 Genetic Encoding

For the encoding of the fully convolutional sub-network, we adapt a CGP based approach (Suganuma et al., 2017) which uses the functional modules described in **Table 1** as the node functions. The fully-connected sub-network is represented using a list of node functions drawn from a function set of dense layers. Thus, the genotype may be considered as the combination of a CGP grid - where each element of

the grid contains a function gene as well as a connection gene - and a list of fully-connected node functions.

The combination of these two encodings is expressed as a directed acyclic graph (DAG). The DAG is an intermediate phenotype which may be adjusted to ensure the validity of networks generated for a given classification task. For the MNIST dataset, we enforce the output layer of each network to be a dense layer with 10 nodes and a softmax activation function.

Finally, the DAG representation is used to construct the CNN, which is implemented as a Keras (Chollet et al., 2015) model. In the remainder of this paper, the CNN is referred to as the phenotype.

### 3.1.1 Representation of the Fully Convolutional Sub-network

The fully-convolutional sub-network is represented using a two-dimensional matrix, in which each element of the matrix contains a string that describes the node function gene as well as the indices of the input nodes. Seven types of node functions are prepared and included in the function set, namely, ConvBlock, ResBlock, DeconvBlock, max pooling, average pooling, concatenation, and summation.

The ConvBlock consists of standard convolution processing with a stride of 1, followed by batch normalization and a ReLU activation function. All convolutions are same convolutions, i.e. the input to the convolution operation is padded with zeros, resulting in an output that matches the input in terms of height and width of the activation map. Thus, the height and width of an activation map is reduced only through pooling layers. The function set contains ConvBlocks of different numbers of output channels and kernel sizes. ResBlocks are composed of ConvBlocks followed by a second convolution operation, batch normalization, summation, and finally ReLU activation. DeconvBlocks consists of a convolution operation followed by batch normalization, ReLU activation, and finally upsampling by a factor of 2.

The max pooling and average pooling functions are applied over a window size of 2, using a stride value of 2. The concatenation function takes two activation maps as input, and concatenates them along the feature axis. In the case where the two activation maps have unequal height and width, the larger activation map is downsampled by max pooling prior to concatenation. Finally, the summation function is used to add the values of two activation maps. In cases where direct summation is not possible due to incompatible numbers of channels in the activation maps, the number of channels in the smaller of the two acti-

vation maps is increased by applying 1-by-1 convolution prior to summation.

### 3.1.2 Representation of the Fully-connected Sub-network

The fully-connected sub-network is represented as a list of DenseBlock node functions as described in **Table 1**. This network is then appended to the output of the fully convolutional sub-network. As mentioned above, a softmax output layer with 10 nodes is appended to the end of the fully-connected network. **Figure 1** illustrates the genotype of the fittest solution obtained by the proposed method.

## 3.2 Evolutionary Algorithm

Evolutionary strategies belong to the family of evolutionary algorithms and are majorly applied to optimization problems. The search paradigm inspired by biological evolution involves applying mutation, recombination and selection operators to a population of candidate solutions. In our work, we adopt the  $(20 + \lambda)$  evolutionary strategy to evolve CNN architectures. We use a value of  $\lambda = 16$ . An initial population of 20 individuals is randomly generated subject to initialization constraints which ensure that the resulting CNNs will fit in the available GPU memory.

### 3.2.1 Mutation Operators

Variation in the population is introduced through mutation of function and connection genes – that is, a given node may have its function swapped with a random selection from the function set, or may have its immediate neighbours swapped.

### 3.2.2 Fitness Evaluation

Each individual is trained on the MNIST training set for 5 epochs, after which it is evaluated on the held-out validation set. It should be noted that the test set is not used for evaluation during evolution. Training hyperparameters are kept constant for all individuals. We use the Adam optimization algorithm (Kingma and Ba, 2017) to minimize Categorical Cross-Entropy loss. A learning rate of  $1e-4$  is used during training for all individuals.

The partially trained networks are then evaluated using the  $F_1$  score, defined in (1), where TP: true positive, FP: false positive, FN: false negative:

$$F_1 = \frac{TP}{(TP + \frac{1}{2}(FP + FN))} \quad (1)$$

Table 1: Node functions present in the CGP function set. F: number of filters (output channels), K: kernel size, N: number of units in a dense layer.

Sub-Network	Node Type	Variation
Fully-Convolutional Network	ConvBlock	$F = \{1, 2, 4, 8, 16, 32, 64, 128, 256, 512, 1024\}$ $K = \{1, 3, 5\}$
	ResBlock	
	DeconvBlock	
	Pooling	Average pooling, Max pooling
	MergeBlock	Summation, Concatenation
Fully-Connected Network	DenseBlock	$N = \{8, 16, 32, 64, 128, 256, 512, 1024, 2048, 4096\}$

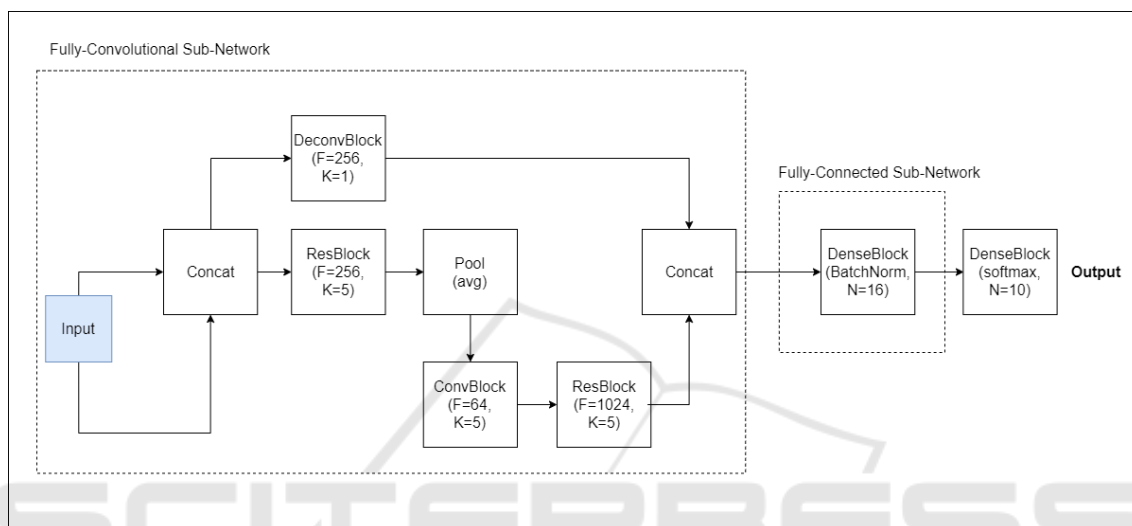


Figure 1: Genotype of the best performing CNN architecture obtained by the proposed method. The figure demonstrates how the active path of the CGP genotype is expressed, resulting in an encoding that describes the CNN in terms of the highly functional modules enumerate in Table 1.

### 3.2.3 Parent Selection and Survivor Selection

For parent selection, we use tournament selection (Miller and Goldberg, 1995) from the current generation with a window size of 5. We select 20% of the population without replacement. For survivor selection, we use tournament selection from the pool of parents and offspring of the current generation, without replacement. A window size of 5 is used. We favour individuals with smaller model size, where model size is defined as the number of trainable parameters of a CNN. Thus, when comparing two individuals, the lesser fit of the two may be selected if: (1) its fitness lies within a tolerance of 0.05 of the fitter individual, and (2) it has fewer trainable parameters than the fitter individual. In the case of the second population, survivor selection is realised in a similar manner: the first clause is the same as above. The second clause is amended to favour individuals with a higher novelty score: the lesser fit of two individuals may be selected if it has fewer trainable parameters, or has a higher novelty score, than the fitter individual.

### 3.2.4 Offspring Generation

Offspring are generated from parents using the aforementioned mutation operators. In the case that a child is produced via a mutation that does not alter the active path (the longest list of connected nodes) its fitness is set equal to that of its parent.

### 3.2.5 Termination Criteria

Evolution is terminated after 200 generations, resulting in 3204 fitness evaluations.

## 3.3 Diversity Measures and Novelty Search

In order to study the effect of structural diversity on the efficiency of the evolutionary algorithm in obtaining optimal solutions, a second population is generated using the Novelty Search algorithm (Lehman and Stanley, 2011). The resulting population is then used as the initial population for the evolutionary algorithm, following the procedure described in the pre-

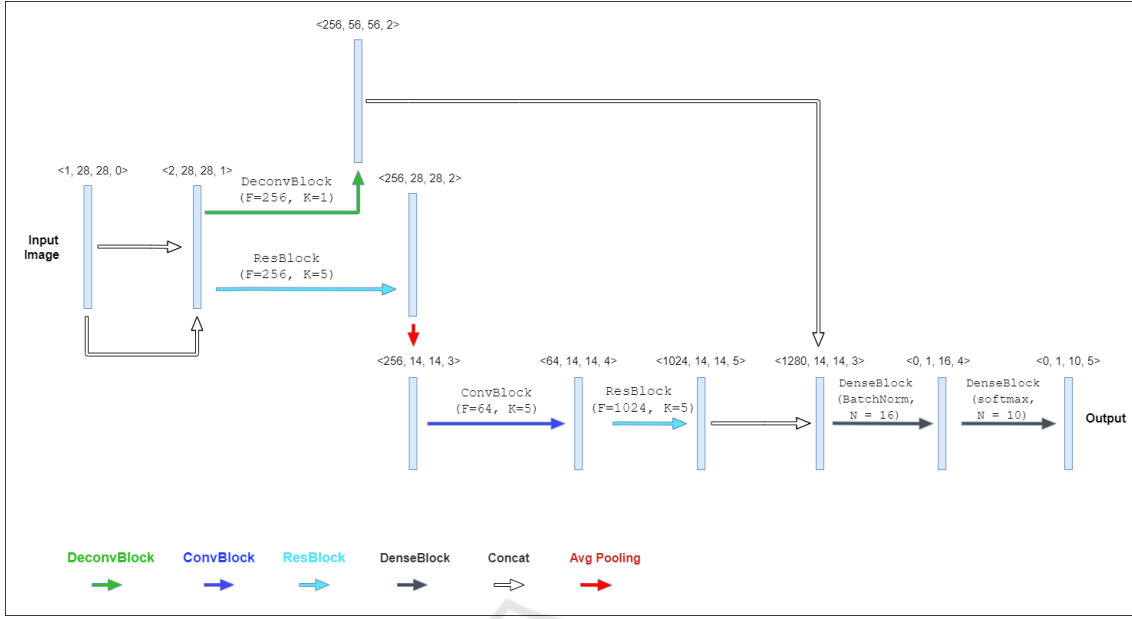


Figure 2: Phenotype of the best performing CNN architecture obtained by the proposed method, with the vector representation of each layer indicated. The figure illustrates the functions of each of the modules represented in the genotype illustrated in Figure 1. The coloured arrows indicate the various functions: DeconvBlock (green), ConvBlock (blue), ResBlock (cyan), DenseBlock (dark gray), Concatenation (white), and Average Pooling (red).

vious section. This is the aforementioned Population 2.

We develop a novelty metric based on cosine similarity as defined below. This metric is used in our Novelty Search algorithm to explore the solution space.

### 3.3.1 Vector Representation of the CNN

The structural information in the phenotype of candidate solutions is represented using sets of 4-dimensional vectors, where each vector represents a successive layer of the CNN. This is illustrated in **Figure 2**. A single layer,  $v_i$ , in a CNN architecture can be represented as in (2).

$$v_i = \begin{pmatrix} c_i \\ x_i \\ y_i \\ d_i \end{pmatrix} \quad (2)$$

Where  $c_i$ ,  $x_i$  and  $y_i$  describe the size of the layer's activation in terms of the numbers of channels, the width, and the height, respectively. The parameter  $d_i$  represents the depth of the layer, i.e., the minimum number of layers between this layer and the input layer.

This representation allows us to obtain an approximate measure of the structural similarity between so-

lutions using vector similarity measures such as cosine similarity.

### 3.3.2 Cosine Similarity and K Nearest Neighbours Computation

The cosine similarity between two vectors is defined as in (3).

$$\text{cosine\_similarity}(v_1, v_2) = \frac{\mathbf{v}_1 \cdot \mathbf{v}_2}{(|\mathbf{v}_1| |\mathbf{v}_2|)} \quad (3)$$

The similarity between two individuals is computed as described by **Algorithm 1**. The novelty of an individual is then calculated using the normalized sum of its similarity with its  $k$  nearest neighbours (Cover and Hart, 1967), with  $k=11$ . This value is then scaled by a factor of 100, and the result is subtracted from 100. Thus, novelty scores lie within the range of 0-100.

### 3.4 Local Optimization

The proposed method involves the use of EAs for exploration and the use of an SLS algorithm for the local optimization of near-optima. In order to demonstrate this procedure, we select from Populations 1 and 2 the generations with highest mean novelty, as illustrated in **Figure 3**. The novelty score of an individual is as defined in Section 3.3.2. Thus, every architecture in

Algorithm 1: Computing similarity between two individuals.

---

```

Result: norm_sum
V1: vector set representation of individual 1
V2: vector set representation of individual 2
similarity: array of length max(length(V1),
length(V2))
norm_sum: normalized element-wise sum of
similarity array
V1 = V1[1:length(V1)-1];
V2 = V2[1:length(V2)-1];
if length(V2) > length(V1) then
    temp ← V1;
    V1 ← V2;
    V2 ← temp;
end
for i ← 0 to length(V1) - length(V2) do
    | V2.append([0,0,0,0])
end
for i ← 0 to length(V1) do
    if norm(V2) = 0 then
    | similarity[i] ← 0;
    else
    | similarity[i] ←
    | cosine_similarity(V1[i], V2[i]);
    end
end
norm_sum ←
sum(similarity)/length(similarity)

```

---

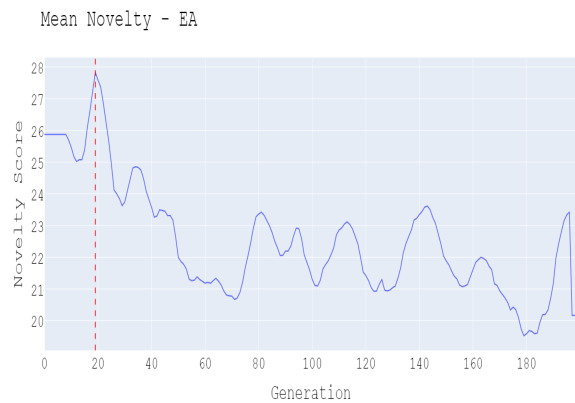
each of these sampled generations contains an evaluation score ( $F_1$  Score) and a novelty score. Based on these two metrics, we select individuals which are determined to be located near/at local optima. We then perform an extensive search of their local neighborhood to discover optimal architectures.

Here, we distinguish two other populations: the group of individuals selected for local optimization from Population 1 is henceforth referred to as Population 3. Similarly, the group of individuals selected from Population 2 will be referred to as Population 4.

### 3.4.1 Identification of Local Optima

As every architecture has an evaluation metric and a novelty metric, the sampling of local optima can be treated as a multi-objective optimization problem. Among the many existing evolutionary algorithms for multi-objective optimization, we use the NSGA-II algorithm. NSGA-II has evolved over the last few years with many new variants (D'Souza et al., 2010) which have reduced its time-complexity or/and improved its convergence to the true Pareto Optimal front.

The algorithm proceeds by performing a non-dominated sorting of the CNN structures based on



(a) Variation of mean novelty over different generations of the evolutionary algorithm for Population 1.

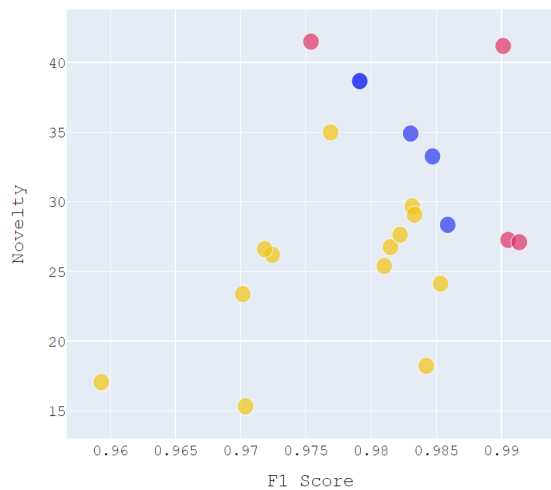


(b) Variation of mean novelty over different generations of the evolutionary algorithm for Population 2, which is optimized for fitness and novelty.

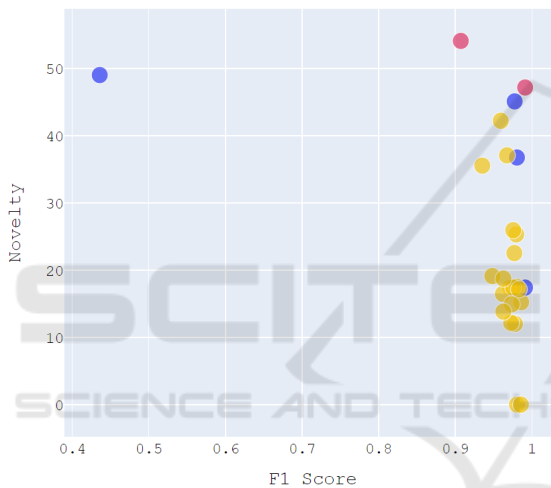
Figure 3: Mean novelty vs time: evolutionary algorithm (top) and evolutionary algorithm with Novelty Search (bottom). In each case, the vertical line indicates the generation selected for local optimization.

their multi-objective fitness values, and ranking the solutions into different non dominated fronts as in **Figure 4**. Thereafter, we sample the solutions by selecting those individuals belonging to the highest ranked front first, followed by those of the next front and so on, until we have obtained at least 4 individuals. In case there is space only for part of a front in the new population, we use a crowded-distance operator to determine the individuals that are from the least crowded regions within that front. Details of the crowded-distance operator can be obtained from (Deb et al., 2002).

The solutions sampled from Population 1 comprise rank 1 and rank 2 solutions, while the four solutions sampled from Population 2 comprise rank 1 solutions only. These constitute the Population 3 and 4, respectively.



(a) Pareto Optimal Front for Population 1.



(b) Pareto Optimal Fronts for Population 2.

Figure 4: The generation with the highest mean novelty score that is sampled from Population 1 and Population 2 is fed into the NSGA II algorithm. The solutions in pink belong to rank 1, solutions in blue belong to rank 2 and solutions in yellow belong to further lower ranks.

### 3.4.2 Simulated Annealing

The solutions found by NSGA II are fed into a local search optimizer. A local search algorithm explores the neighborhood of a candidate by comparing it with neighboring solutions. This search is guided by a cost function that measures the quality of a given solution.

In our work, we have chosen Simulated Annealing as the local optimization algorithm. Simulated Annealing is a heuristic method which was inspired by the physical annealing of metals (Kirkpatrick et al., 1983). The search algorithm iteratively compares a given solution to another neighboring solution in the local neighborhood of the current solution. The cost

function reflects the difference between the fitness of the current solutions and that of a neighbour. If the cost is positive (neighbour is fitter), the algorithm selects the neighboring solution as the (working) optimal one for the next iteration. However, if the cost is negative, the algorithm selects either solution (current or neighbour), on a probabilistic basis described by (4).

$$P = \exp\left(\frac{cost}{T}\right) \quad (4)$$

The algorithm starts with an initial 'high temperature', when the probability of accepting bad solutions is higher. This ensures that the algorithm does not get stuck in a local optimum. The temperature is iteratively reduced in line with a cooling schedule. The most popular cooling schedule is the geometric cooling schedule, which defines a parameter  $\alpha$  with a value between 0 and 1. At the conclusion of every iteration, the temperature is updated in line with (5).

$$T = \alpha * T \quad (5)$$

As the algorithm progresses the temperature decreases exponentially according to the cooling schedule, making the algorithm more greedy. Thus the probability of choosing solutions with lower fitness decreases with increasing iterations. Simulated annealing terminates after a fixed number of iterations and yields the most optimal solutions from the local neighborhood of the initial candidate solutions. We have chosen an initial temperature of 1000, with  $\alpha = 0.91$ . The algorithm terminates after 183 iterations when the final value of temperature is 0.000032155.

### 3.4.3 Estimation of Local Neighborhood

To define the neighborhood function we use the cosine similarity metric defined in (3). We compute the cosine distance between the generated neighbor, produced by mutating a candidate solution, and every other individual in the population. The mutated individual is then assigned to the neighborhood of the candidate solution with which it has the highest similarity.

## 3.5 Experimental Setting

The MNIST (LeCun and Cortes, 2010) data-set is a set of 28x28 pixel gray-scale images of handwritten digits. It consists of 60,000 training images and 10,000 test images. In our experiments, we split the training images into a training set of 50,000 images and a held-out validation set of 10,000 images. Image pixel values are normalized by dividing each value by 255.

All experiments are conducted on machines with the following features: two Intel E5-2650 v4 Broadwell 2.2GHz CPUs with 24 CPU cores, four NVIDIA P100 Pascal 16 GB GPUs, and 128 GB RAM.

## 4 RESULTS

Using the methods described in the preceding section, we develop four distinct populations of CNNs:

1. Population 1: the population obtained using the standard evolutionary algorithm.
2. Population 2: the population obtained using the evolutionary algorithm with Novelty Search initialization.
3. Population 3: the population obtained from the standard evolutionary algorithm and subsequent local optimization via Simulated Annealing.
4. Population 4: the population obtained from the evolutionary algorithm with Novelty Search initialization and subsequent local optimization via Simulated Annealing.

From each of these populations, the fittest four individuals are selected and trained completely using the 50,000 images from the MNIST data-set reserved for training. The held-out validation data-set is used to prevent over-fitting by applying the early stopping regularization method (Caruana et al., 2000). Each network is trained for up to 100 epochs, with an early stopping patience parameter of 20 epochs.

The trained networks are then evaluated on the previously unseen 10,000 test images. The resulting recognition error is reported in **Table 2** along with the number of trainable parameters. The number of fitness evaluations completed before obtaining each solution is also reported. The minimum error obtained by any individual across all populations is 0.48%, and was found in population 4.

### 4.1 Recognition Error

From the results over the four populations, we can observe that individuals from each population obtained competitive recognition errors. However, the large discrepancy in performance between the fittest and fourth fittest individuals obtained by the EA alone (Population 1) suggests a failure by the EA in exploiting the many peaks of the fitness landscape, simultaneously. The variance in recognition error of the four best individuals obtained by the EA alone is 0.0169.

When novelty is included as an objective in Population 2, we observe a slight reduction in performance in terms of fitness value and recognition error.

The four best individuals in this case exhibit approximately equal performance. Since they have high novelty scores, it is reasonable to infer that they belong to distinct regions within the solution space. In this case, the variance in recognition error is 0.0013.

Populations 3 and 4 are obtained through local optimization. Recall that during local optimization, each individual is constrained from entering the neighbourhood of the solution space occupied by any of the other individuals in the population. An inspection of the recognition errors reveals that some individuals in Population 3 have become constrained to sub-optimal regions of the solution space, when compared to individuals in Population 4. In addition, the variances in recognition error exhibited by these two populations are 0.0172 and 0.0025, respectively.

From the discussion above, it appears that the inclusion of novelty as a search objective results in a reduction in the variance of recognition error, by an order of magnitude. This suggests that, by enforcing exploratory behaviour, our method discovers highly-fit solutions that come from different parts of the solution space- resulting in a highly diverse *and* highly fit set of solutions.

### 4.2 Number of Fitness Evaluations

Here, we conduct a comparison of the number of fitness evaluations required to obtain optimal solutions in each of the four populations. Similarly to our discussion on the variance of recognition errors, we consider the mean and standard deviation of the number of fitness evaluations required to obtain the four best solutions for each of the four populations. For populations 1 through 4, these values are  $1655 \pm 1260$ ,  $2986 \pm 204$ ,  $905 \pm 111$ , and  $1030 \pm 46$  fitness evaluations, respectively. The average time taken for each fitness evaluation was found to be 3.12 minutes per evaluation.

The populations obtained through local optimization via Simulated Annealing appear to require fewer fitness evaluations in order to obtain optimal solutions, compared to those obtained through the evolutionary approach ( $p < .05$ ). This is further illustrated by **Figure 5**, which demonstrates that the evolutionary algorithms incur a large number of wasted cycles in between discoveries of optimal solutions. This is in contrast to **Figure 6**, which illustrates the ability of the Simulated Annealing algorithm to rapidly climb towards local optima. This is especially salient after approximately 600 fitness evaluations, when the temperature of the cooling schedule has reduced, and the algorithm has become more deterministic.

Table 2: Summary of the four fittest individuals obtained from each population. Individuals are sorted by test error. Populations 1 through 4 are as described in the preceding sections, and reiterated in Section 4.

Population	Individual #	# Trainable Parameters	# Fitness Evaluations	Fitness Score	Test Error (%)
Population 1	1	5.493 M	2676	0.992	0.57
	2	0.968 M	3104	0.987	0.69
	3	9.175 M	136	0.990	0.71
	4	103.364 M	704	0.989	0.93
Population 2	1	850.491 M	2746	0.993	0.64
	2	1.018 M	3158	0.987	0.72
	3	0.232 M	3217	0.989	0.72
	4	7.358 M	2821	0.985	0.73
Population 3	1	7.400 M	1004	0.994	0.67
	2	14.488 M	964	0.993	0.52
	3	32.219 M	716	0.992	0.83
	4	19.118 M	936	0.992	0.84
Population 4	1	34.011 M	1072	0.994	0.48
	2	46.063 M	1024	0.993	0.54
	3	7.550 M	956	0.992	0.57
	4	8.863 M	1068	0.992	0.62

Lastly, the lower variance exhibited by populations 3 and 4 suggests that the local optimization approach will reliably obtain optimal solutions within a narrow range of number of fitness evaluations.

### 4.3 Comparison to Related Works

The proposed method obtains competitive performance in terms of recognition error on the MNIST test data-set. However, the trained networks obtained by our method do not rival the state-of-the-art. During training, it was observed that the early stopping technique halted training well before 100 epochs. Further improvements may be obtained by including other regularization techniques, such as the inclusion of dropout layers (Srivastava et al., 2014). A comparison to related works is provided in **Table 3**.

## 5 CONCLUSIONS AND FUTURE WORK

In this paper, we have investigated the use of a three-stage CGP-based hybrid evolutionary algorithm (EA) for the training of CNNs, used for handwritten digit recognition. The well-known MNIST data-set is used to assess the performance of the trained CNNs.

The first stage is meant to generate a population of diverse CNNs, and for that reason we propose a method for measuring structural similarity between CNN architectures. The second stage increases the fitness of the population (while not sacrificing diver-

Table 3: Comparison of the recognition error (%) on the MNIST test dataset to related works.

Model	MNIST (%)
psoCNN (Fernandes Junior and Yen, 2019)	0.32
GeNet (Xie and Yuille, 2017)	0.36
HyperNEAT with CNN (Verbancsics and Harguess, 2015)	7.90
evoCNN (Sun et al., 2019)	1.18
IPPSO (Wang et al., 2018)	1.13
(Baldominos et al., 2018)	0.37
Our method	0.48

sity) by means of artificial evolution. Most critically, we demonstrate how the final stage of the proposed methodology (simulated annealing) is able to optimize the potential locally optimal individuals found in previous stages, and do so more efficiently than a non-hybridized EA.

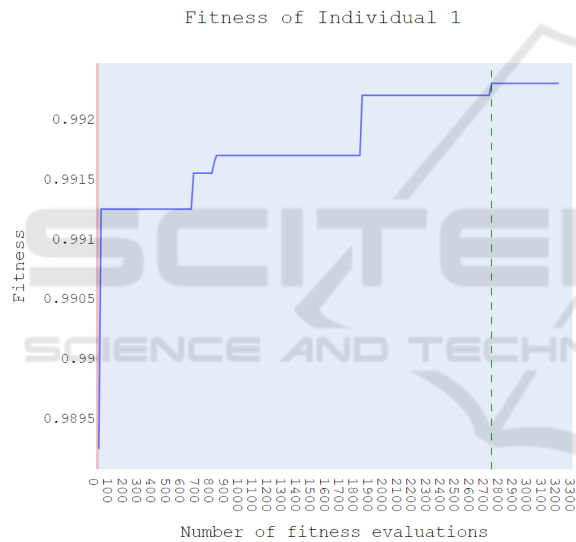
The results of our experiments suggest that the proposed method *reduces*, and *reliably*, the computational effort needed for obtaining optimal solutions, compared to a standard evolutionary approach. We quantify computational effort in terms of the number of fitness evaluations required to obtain optimal solutions. The number of fitness evaluations required by the proposed method was found to be significantly fewer than the number required by the standard EA ( $p < .05$ ).



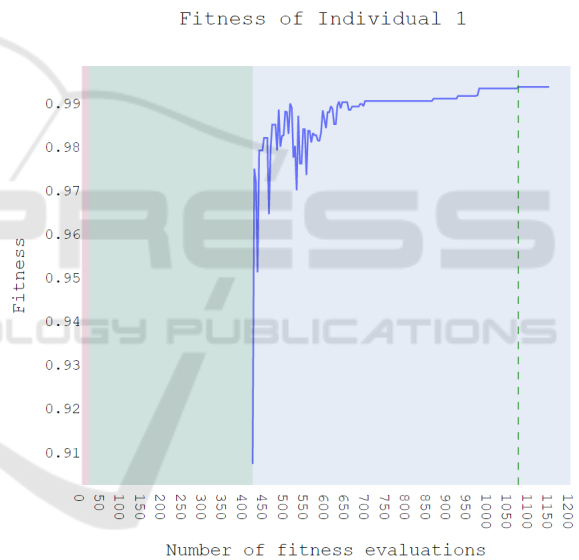
(a) Fitness of Individual 1 from Population 1.



(a) Fitness of Individual 1 from Population 3.



(b) Fitness of Individual 1 from Population 2.



(b) Fitness of Individual 1 from Population 4.

Figure 5: The above figures indicate the variation of fitness over number of fitness evaluations during the evolutionary process for Populations 1 and 2. The best fitness for (5a) is obtained after 2676 evaluations and that for (5b) is obtained after 2746 evaluations. The shaded red region represents the number of fitness evaluations during the initialization of the population.

In addition, we have observed that including novelty as an objective has the effect of *reducing* the variance of recognition errors by an order of magnitude compared to the pure evolutionary approach. The proposed method involves optimizing individual solutions within a constrained local neighbourhood. Thus, we infer from this result that the proposed method effectively obtains optimal solutions belonging to *different* regions of the solution space.

Figure 6: The above figures indicate the variation of fitness over the local optimization process for Populations 3 and 4. The best fitness for (6a) is obtained after 1004 evaluations and that for (6b) is obtained after 1072 evaluations, during the optimization phase. The shaded red region represents the number of fitness evaluations during the initialization and the green region represents the number of fitness evaluations during the evolutionary process until sampling is done.

The best recognition error obtained by our method on the MNIST test data-set was found to be 0.48%. In comparison to related works, this reflects *competitive* performance. However, some peer competitors have obtained recognition error as low as 0.32%. In order to *improve* performance of the CNNs evolved using

our CGP framework, we recommend the investigation of regularization techniques, such as dropout. Also, the evolution of recurrent structures within the CNNs may be explored for improved performance.

Future work may explore measures of structural similarity which act on the DAG representation of CGP genotype, such as Graph Edit Distance (Sanfeliu and Fu, 1983). In addition, the method may be applied to other CNN tasks such as image segmentation. Lastly, an investigation of alternative SLS algorithms may yield further improvements in terms of reduced computational cost.

## ACKNOWLEDGEMENTS

We acknowledge the support of the Natural Sciences and Engineering Research Council of Canada (NSERC).

## REFERENCES

- Baldominos, A., Saez, Y., and Isasi, P. (2018). Evolutionary convolutional neural networks: An application to handwriting recognition. *Neurocomputing*, 283:38–52.
- Caruana, R., Lawrence, S., and Giles, L. (2000). Overfitting in neural nets: Backpropagation, conjugate gradient, and early stopping. NIPS'00, page 381–387, Cambridge, MA, USA. MIT Press.
- Chollet, F. et al. (2015). Keras. <https://keras.io>.
- Cover, T. and Hart, P. (1967). Nearest neighbor pattern classification. *IEEE Transactions on Information Theory*, 13(1):21–27.
- Deb, K., Pratap, A., Agarwal, S., and Meyarivan, T. (2002). A fast and elitist multiobjective genetic algorithm: Nsga-ii. *IEEE Transactions on Evolutionary Computation*, 6(2):182–197.
- D'Souza, R., Sekaran, C., and Kandasamy, A. (2010). Improved nsga-ii based on a novel ranking scheme. *Journal of Computing*, 2.
- Fernandes Junior, F. E. and Yen, G. G. (2019). Particle swarm optimization of deep neural networks architectures for image classification. *Swarm and Evolutionary Computation*, 49:62–74.
- Kingma, D. P. and Ba, J. (2017). Adam: A method for stochastic optimization.
- Kirkpatrick, S., Gelatt, C. D., and Vecchi, M. P. (1983). Optimization by simulated annealing. *Science*, 220(4598):671–680.
- Lecun, Y., Bottou, L., Bengio, Y., and Haffner, P. (1998). Gradient-based learning applied to document recognition. *Proceedings of the IEEE*, 86(11):2278–2324.
- LeCun, Y. and Cortes, C. (2010). MNIST handwritten digit database.
- Lehman, J. and Stanley, K. O. (2011). Novelty search and the problem with objectives. In Riolo, R., Vladislavleva, E., and Moore, J. H., editors, *Genetic Programming Theory and Practice IX*, pages 37–56. Springer New York, New York, NY.
- McGhie, A., Xue, B., and Zhang, M. (2020). Gpcnn: evolving convolutional neural networks using genetic programming. In *2020 IEEE Symposium Series on Computational Intelligence (SSCI)*, pages 2684–2691, Canberra, ACT, Australia. IEEE.
- Miller, B. and Goldberg, D. (1995). Genetic algorithms, tournament selection, and the effects of noise. *Complex Syst.*, 9.
- Miller, J. F. and Thomson, P. (2000). Cartesian genetic programming.
- Sanfeliu, A. and Fu, K.-S. (1983). A distance measure between attributed relational graphs for pattern recognition. *IEEE Transactions on Systems, Man, and Cybernetics*, SMC-13(3):353–362.
- Srivastava, N., Hinton, G., Krizhevsky, A., Sutskever, I., and Salakhutdinov, R. (2014). Dropout: a simple way to prevent neural networks from overfitting. *The journal of machine learning research*, 15(1):1929–1958.
- Stanley, K. O., D'Ambrosio, D. B., and Gauci, J. (2009). A Hypercube-Based Encoding for Evolving Large-Scale Neural Networks. *Artificial Life*, 15(2):185–212.
- Stanley, K. O. and Miikkulainen, R. (2002). Evolving Neural Networks through Augmenting Topologies. *Evolutionary Computation*, 10(2):99–127.
- Suganuma, M., Shirakawa, S., and Nagao, T. (2017). A genetic programming approach to designing convolutional neural network architectures. In *Proceedings of the Genetic and Evolutionary Computation Conference*, pages 497–504, Berlin Germany. ACM.
- Sun, Y., Xue, B., Zhang, M., Yen, G. G., and Lv, J. (2020). Automatically designing cnn architectures using the genetic algorithm for image classification. *IEEE Transactions on Cybernetics*, 50(9):3840–3854.
- Sun, Y., Yen, G. G., and Yi, Z. (2019). Evolving unsupervised deep neural networks for learning meaningful representations. *IEEE Transactions on Evolutionary Computation*, 23(1):89–103.
- Verbancsics, P. and Harguess, J. (2015). Image classification using generative neuro evolution for deep learning. In *2015 IEEE Winter Conference on Applications of Computer Vision*, pages 488–493.
- Wang, B., Sun, Y., Xue, B., and Zhang, M. (2018). Evolving deep convolutional neural networks by variable-length particle swarm optimization for image classification. In *2018 IEEE Congress on Evolutionary Computation (CEC)*, pages 1–8.
- Xie, L. and Yuille, A. (2017). Genetic cnn. In *2017 IEEE International Conference on Computer Vision (ICCV)*, pages 1388–1397, Venice. IEEE.